

# Time-resolved photometric and spectroscopic analysis of the luminous Ap star HD 103498

S. Joshi,<sup>1\*</sup> T. Ryabchikova,<sup>2,3</sup> O. Kochukhov,<sup>4</sup> M. Sachkov,<sup>2</sup> S. K. Tiwari,<sup>1</sup>  
N. K. Chakradhari<sup>5</sup> and N. Piskunov<sup>4</sup>

<sup>1</sup>*Aryabhata Research Institute of Observational Sciences (ARIES), Manora Peak, Nainital, India*

<sup>2</sup>*Institute of Astronomy, Russian Academy of Sciences, Pyatnitskaya 48, 119017 Moscow, Russia*

<sup>3</sup>*Institut für Astronomie, Universität Wien, Türkenschanzstrasse 17, 1180 Wien, Austria*

<sup>4</sup>*Department of Physics and Astronomy, Uppsala University, SE-751 20 Uppsala, Sweden*

<sup>5</sup>*School of Studies in Physics and Astrophysics, Pt. Ravishankar Shukla University, Raipur, India*

Accepted 2009 September 16. Received 2009 September 14; in original form 2009 June 25

## ABSTRACT

We present the results of the photometric and spectroscopic monitoring of the luminous Ap star HD 103498. The time-series photometric observations were carried out on 17 nights using a three-channel fast photometer attached to the 1.04-m optical telescope at the Aryabhata Research Institute of Observational Sciences (ARIES), Nainital. The photometric data from five nights in 2007 show a clear signature of 15-min periodicity. However, the follow-up observations during 2007–2009 did not reproduce any such periodicity. To confirm the photometric light variations, time-series spectroscopic observations were carried out with the 2.56-m Nordic Optical Telescope (NOT) at La Palma on 2009 February 2. No radial velocity variations were present in this data set, which is in full agreement with the photometric observations taken around the same date. Model atmosphere and abundance analysis of HD 103498 show that the star is evolved from the main sequence and its atmospheric abundances are similar to those of two other evolved Ap stars, HD 133792 and HD 204411: large overabundances of Si, Cr and Fe and moderate overabundances of the rare-earth elements. These chemical properties and a higher effective temperature distinguish HD 103498 from any known roAp star.

**Key words:** stars: individual: HD 103498 – stars: magnetic fields – stars: oscillations – stars: variables: others.

## 1 INTRODUCTION

The chemically peculiar (CP) star HD 103498 (65 UMa D, HR 4561) is a member of a multiple system that consists of four objects. According to Pourbaix et al. (2004), HD 103498 is the south-eastern component of the visual binary ADS 8347 (separation 63 arcsec) containing HR 4561 and HR 4560, with the latter being the spectroscopic binary 65 UMa AC. Abt & Morrell (1995) classified it as CrSrEu based on a low-resolution Cassegrain photographic spectrum. The first magnetic field measurements of 65 UMa D were reported by Glagolevskij et al. (1985), who discovered a strong negative longitudinal magnetic field ( $B_z$ ) of about  $-630$  G. Using the MuSiCoS spectropolarimeter attached to the 2.0-m Telescope Bernard Lyot (TBL) at Observatoire du Pic du Midi, France, Aurière et al. (2007) measured a much weaker longitudinal field ( $B_z$ ) that varied between  $\pm 200$  G with a period of 15.83 days. The authors derived a rotational velocity of  $v_e \sin i = 13 \text{ km s}^{-1}$  and estimated

an effective temperature  $T_{\text{eff}} = 9220 \pm 300$  K and luminosity  $\log(L/L_{\odot}) = 2.06 \pm 0.20$  for the star.

The Strömgren indices of HD 103498 are  $b - y = 0.003$ ,  $m_1 = 0.196$ ,  $c_1 = 1.010$  and  $H\beta = 2.858$  (Hauck & Mermilliod 1998). On the basis of the peculiar indices and Ap spectral classification, HD 103498 was observed using a high-speed photometric technique as part of a survey programme searching for photometric variability in CP stars. Tiwari, Chaubey & Pandey (2007) reported a 15-min periodic oscillation with varying amplitude from night to night. The location of this star in the HR diagram (see Fig. 8), towards a greater luminosity and higher temperature than any roAp star observed until now, makes it an unusual pulsator. Therefore, we continued to monitor this star photometrically. In addition, we obtained the time-series spectroscopy to search for possible rapid radial velocity (RV) variations, because in almost all known roAp stars the RV amplitudes exceed the photometric amplitudes significantly and the pulsational signal may be detected in RV with no detection in the photometry (Hatzes & Mkrtychian 2004 –  $\beta$ CrB; Kochukhov et al. 2009 – HD 75445).

This paper presents the combined results from the photometric and spectroscopic observations of HD 103498 and is organized as

\*E-mail: santosh@aries.res.in

follows. The photometric observations and data analysis are described in Section 2. The results obtained from the high-resolution spectroscopy are presented in Section 3. In Section 4 the implications of variability are discussed, and the conclusions drawn from these observations are outlined in Section 5.

## 2 PHOTOMETRIC OBSERVATIONS AND DATA ANALYSIS

In the search for photometric light variations in short-period ( $\sim$ min) pulsating variables, high-speed photometry is an established technique that has been used since the 1980s. The high-speed photometric observations of HD 103498 were obtained using a three-channel fast photometer attached to the 1.04-m Sampurnanand telescope of the Aryabhata Research Institute of Observational Sciences (ARIES), which is located at an altitude of  $\sim$ 1950 m above sea level at a longitude of  $79^{\circ}27'E$  and latitude of  $29^{\circ}22'N$ , and has an average full width at half-maximum (FWHM) seeing of the order of 2 arcsec (Ashoka et al. 2001; Sagar 1999). We obtained time-series photometric data through a Johnson *B*-filter with an integration of 10 s each for a total duration of 36 h (Table 1). An aperture of 30 arcsec was used to minimize flux variations caused by seeing fluctuations and guiding. The centring of the star was checked using manual guiding in a non-periodic time-interval. The data reduction process involved the following steps: (i) visual inspection of the light curve to identify and remove the bad data points; (ii) correction for coincident counting losses; (iii) subtraction of the interpolated sky background; and (iv) correction for the mean atmospheric extinction. After applying these corrections, the times of the mid-point of each data point were converted into heliocentric Julian dates (HJD) with an accuracy of  $10^{-5}$  d ( $\sim$ 1 s). The reduced data comprised a time-series of the HJD and  $\Delta B$  magnitudes with respect to the mean values of the run (light curve). The frequency analysis was performed using Deeming's Discrete Fourier Transform (DFT) for unequally spaced data (Deeming 1975). The frequency analysis produces an amplitude spectrum that provides the frequencies,

amplitude and phase that act as input parameters for the subsequent analysis.

HD 103498 has been observed photometrically on a total of 17 nights over the last four years, and Table 1 gives the journal of these observations. The quoted error in the frequency is the FWHM of the peak. The phase ( $\phi$ , in period fractions) is calculated with the ephemeris used in the construction of the magnetic curve by Aurière et al. (2007) and kindly provided by one of the authors, G. Wade:

$$\text{HJD}(\text{magn.max}) = 245\,0000.0 + 15.830\text{ d.}$$

Note that the accuracy of the magnetic period as estimated by Aurière et al. (2007) is  $\pm 0.010$  d, which is not high enough to determine the correct phases of the current photometry and spectroscopy. Expected phase errors are within  $\pm 0.15$ – $0.20$  for the whole data set. Columns 7 and 8 give the signal-to-noise ratio and false alarm probability, respectively. Some of the sample light curves of HD 103498 are shown in Fig. 1, and corresponding amplitude spectra are shown in Fig. 2. The horizontal dotted lines in the frequency spectra correspond to the 98 per cent confidence level according to the criteria of Scargle (1982). The long-term sky-transparency variations in the time-series data were removed by subtracting a sinusoidal function of frequency  $f_1$ , amplitude  $A_1$  and phase  $\phi_1$  of the form  $A_1 \cos(2\pi f_1 t + \phi_1)$ , a technique known as 'prewhitening'. The process was repeated until the sky-transparency peaks were reduced to the level of scintillation noise. The amplitude spectra (Fig. 2) clearly show that the star light remained practically constant towards the end of 2006. A peak appeared at the frequency 1.06 mHz on 2007 March 5, and then faded away on the next night. After an interval of a month the amplitude peaked again, and subsequently dropped on 2007 April 7. On the same night, which had the longest observing run, we found a double peak profile. Further observations did not show any prominent peak at this frequency. The frequency spectra also show amplitude modulations, which are generally observed in roAp stars and might be caused by one or more of the following effects: (i) changing aspects as the star rotates; (ii) beating between unresolved pulsation modes; and (iii) real variations in the amplitude of the mode of pulsation. The detection

**Table 1.** Journal of photometric observations of HD 103498 obtained from ARIES. The HJD is 245 0000+, and '-' in the frequency and amplitude columns indicates no light variations. The magnetic phase  $\phi$  corresponds to  $t_0 = \text{HJD } 245\,0000$ ,  $z$  is the signal-to-noise ratio in power, and  $F$  is the false alarm probability.

Set no.	Start time (HJD)	$\Delta t$ (h)	$f$ (mHz)	$A$ (mmag)	$\phi$ ( $\pm 0.2$ )	$z$	$F$
1	4101.46794	1.44	-	-	0.10		
2	4165.20987	2.74	$1.06 \pm 0.10$	0.95	0.12	22.56	7.84E-8
3	4166.19829	1.85	$1.10 \pm 0.13$	0.49	0.19	9.38	0.0277
4	4196.15852	3.10	$1.18 \pm 0.12$	1.69	0.08	71.40	$\sim 0$
5	4197.12757	1.82	$1.09 \pm 0.17$	1.71	0.14	73.10	$\sim 0$
6	4198.10264	6.33	$1.13 \pm 0.03$	0.81	0.21	16.40	8.59E-5
7	4455.45086	1.03	-	-	0.46		
8	4459.46167	1.35	-	-	0.71		
9	4584.14787	1.22	-	-	0.59		
10	4585.11297	2.10	-	-	0.65		
11	4831.34313	3.24	-	-	0.21		
12	4842.32422	1.83	-	-	0.90		
13	4869.29544	2.11	-	-	0.60		
14	4870.28783	1.71	-	-	0.66		
15	4898.18485	1.95	-	-	0.43		
16	4899.28240	1.97	-	-	0.50		
17	4959.12810	3.53	-	-	0.28		

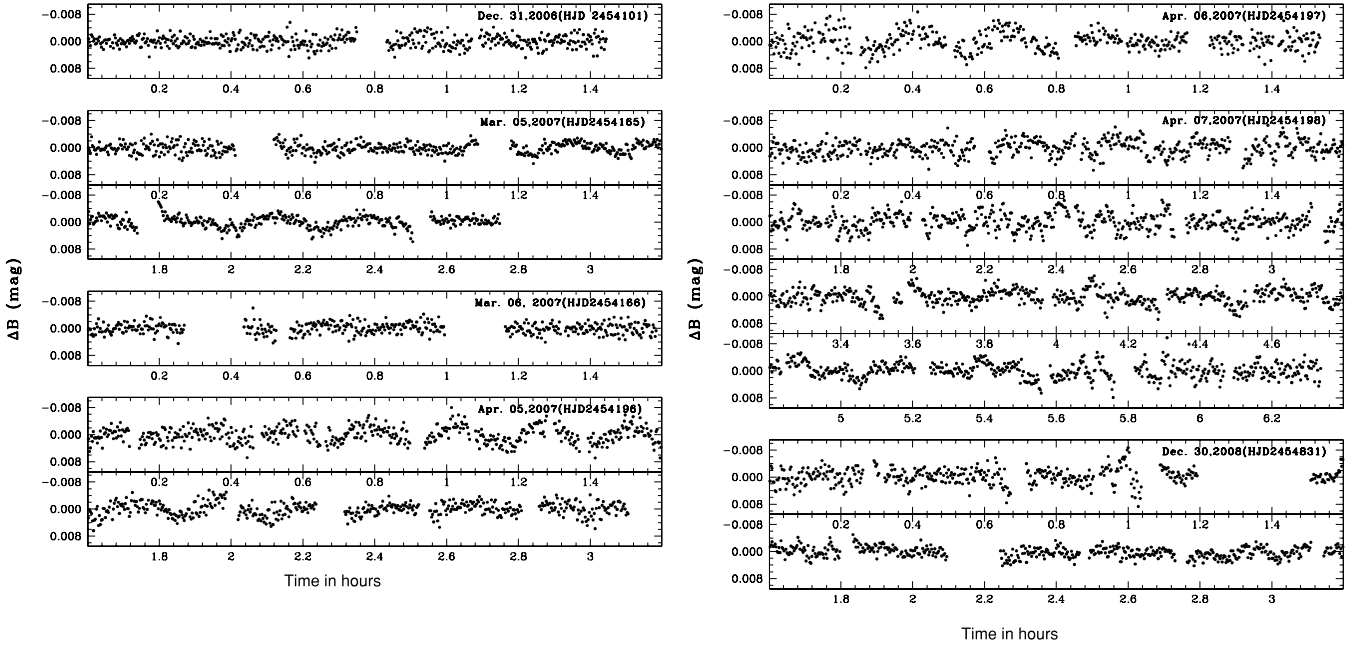


**Figure 1.** Light curves of HD 103498 obtained on various nights between 2006 and 2008. The HJD (245 0000+) of each observation is noted in each panel.

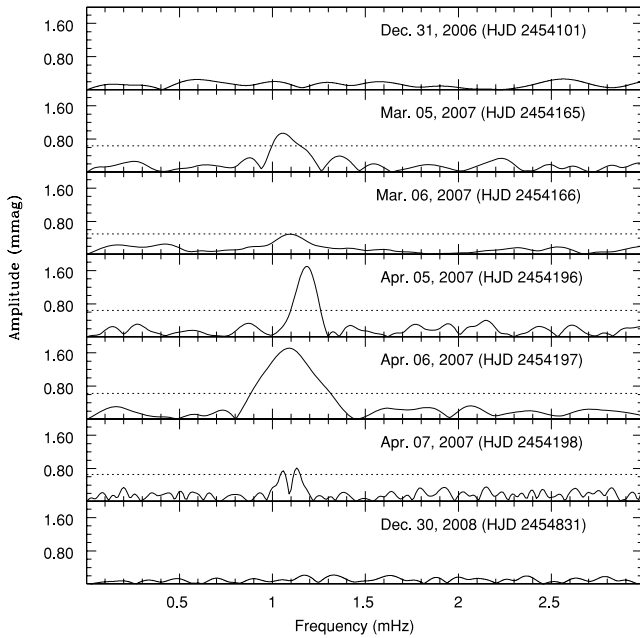


**Figure 2.** The amplitude spectra of the light curves shown in Fig. 1. The dashed lines correspond to the 98 per cent confidence level according to the criteria of Scargle (1982).

of periodic variability in HD 103498 is unlikely to be spurious, as on two observing nights we also observed two non-variables and two known  $\delta$  Scuti stars just before and after HD 103498. Fig. 3 shows the amplitude spectra of these stars along with that of HD 103498. It can be seen that the amplitude spectrum for HD 103498 shows a prominent peak at a frequency of  $\sim 1.1$  mHz, whereas this is absent in the others. The prominent peaks in the amplitude spectra of HD 118660 and HD 113878 correspond to the  $\delta$  Scuti pulsation reported by Joshi et al. (2006).

To check the significance of the variability seen on the five nights, the ‘False Alarm’ criterion of Scargle (1982) was used to find the

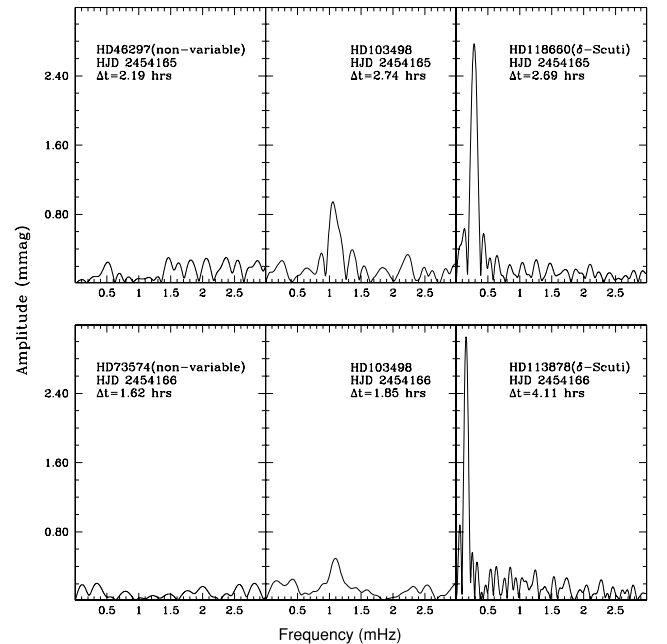


**Figure 3.** Amplitude spectrum of two non-variables and two  $\delta$  Scuti stars observed on the same nights as HD 103498. The peak at frequency  $\sim 1.0$  mHz is absent in all spectra other than HD 103498. The high-amplitude peaks in the  $\delta$  Scuti stars HD 118660 and HD 113878 correspond to the period range of  $\delta$  Scuti stars.

false alarm probability  $F$ . It is expressed as

$$F = 1 - [1 - \exp(-z)]^N, \quad (1)$$

where  $N$  is the number of independent frequencies searched in the time-series. For a given Nyquist frequency  $\nu_N$ ,  $N$  is given as  $\cong \nu_N \Delta t$ , where  $\Delta t$  is the total time-span of the data set. The exponential power ‘ $z$ ’ represents the signal-to-noise ratio in power. We calculated the false alarm probabilities  $F$  for the data sets in which variability was detected. The last column of Table 1 gives the values

of  $F$  for various data sets. The confidence level of the peak on four of the five nights is  $>99$  per cent, the exception being 2007 April 7 (HJD 245 4166), when the level is 97.23 per cent. Therefore, the variability seen in HD 103498 has almost no chance of being an artefact.

### 3 SPECTROSCOPIC ANALYSIS

#### 3.1 Observations and data reduction

To check for possible rapid variability of HD 103498, we performed time-resolved spectroscopy of HD 103498 using a fibre-fed echelle spectrograph (FIES) at the 2.56-m Nordic Optical Telescope (NOT). The observations were obtained for a duration of 3.4 h on the night of 2009 February 2 (HJD 245 4865.624–245 4865.764) as part of the NOT Fast-track Service Mode Program 38–415. We collected 71 stellar spectra, each with an exposure time of 120 s. With the overhead of 48 s this gave us a sampling rate of approximately one spectrum every 168 s, sufficient to resolve the 15-min pulsation period suspected in HD 103498. Our observations fall into the magnetic phase range  $0.37 \pm 0.2$  if the magnetic ephemeris and the error of the period are used.

The FIES instrument was configured to use the medium-resolution mode, which provides a wavelength coverage of the region 3635–7270 Å at a resolving power of  $R = 47000$ . We used the `REDUCE` package of Piskunov & Valenti (2002) to perform the standard steps of the echelle spectra reduction (construction of the master flat-field and bias frames, order location, flat-fielding and wavelength calibration) followed by the optimal extraction of the stellar spectra. The typical signal-to-noise ratio of the individual observations is 80–100 around  $\lambda 5000$ . Individual echelle orders of the extracted spectra were post-processed as described by Kochukhov et al. (2007) to ensure a consistency of the continuum normalization for all 71 spectra. We obtained two ThAr reference spectra, one at the beginning and the other at the end of the stellar time-series. Each arc frame was wavelength-calibrated to an internal precision of 50–60 m s<sup>-1</sup> using  $\approx 1500$  emission lines in all echelle orders. A RV drift of 120 m s<sup>-1</sup> was measured between the two ThAr exposures. This change of the zero point of the spectrograph, as well as a small change of the heliocentric RV that occurred during our observations, was compensated by subtracting a straight-line fit from the RV measurements of the individual lines and spectral regions.

In addition to the FIES data we used one of the MuSiCoS spectra employed for magnetic field measurements (Aurière et al. 2007). This spectrum, kindly provided by G. Wade, was obtained at JD = 245 2255.73 close to the phase of magnetic minimum, with a signal-to-noise ratio of about 200 and a spectral resolution of  $R = 35\,000$ . The details of general data reduction are given in Aurière et al. (2007). For the purpose of our analysis, we re-normalized the continuum slightly.

#### 3.2 Abundance analysis

We performed a full spectroscopic analysis of HD 103498 to identify its evolutionary status and chemical peculiarities. The abundance study of the star was based primarily on the averaged spectrum of our time-series spectroscopy in the spectral region 3900–7270 Å. We repeated the abundance analysis using the MuSiCoS spectrum and obtained results in agreement with those derived from the averaged FIES spectrum within the errors of abundance determination. For hydrogen line profiles we used the MuSiCoS spectrum, for which the continuum is better defined in the region of the line wings.

#### 3.2.1 Fundamental parameters

The atmospheric parameters of HD 103498 were estimated using the calibration of Strömgren (Moon & Dworetzky 1985) and Geneva photometry (Kunzli et al. 1997) realized in the package `TEMPLOGG` (Kaiser 2006). Photometric indices were taken from Hauck & Mermilliod (1998, Strömgren), and from Runefer (1976, Geneva). An average effective temperature  $T_{\text{eff}} = 9370 \pm 140$  K and  $\log g = 3.90$  were obtained. Analysis of H $\alpha$  and H $\beta$  line profiles shows that, although the effective temperature estimate is reliable, the surface gravity is certainly overestimated. A reasonable fit of the calculated H $\alpha$  and H $\beta$  line profiles to the observed ones was obtained with the following atmospheric parameters:  $T_{\text{eff}} = 9500$  K,  $\log g = 3.6$  (Fig. 4). We used these parameters in all subsequent abundance calculations.

To estimate the luminosity we did not use the parallax value of 3.37 mas of the star as given by van Leeuwen (2007) for an individual object. If HD 103498 (65 UMa D) and 65 UMa AC comprise a physical pair (Pourbaix et al. 2004), both stars should have similar parallaxes. Therefore, we adopted a weighted mean parallax value of the entire system,  $4.02 \pm 0.40$  mas, for HD 103498. The reddening parameter  $E(B - V) = 0.007$  and interstellar absorption  $A_V = 0.021$  mag were estimated from the *UBV* photometric data of Huchra & Willner (1973). The derived luminosity of the star,  $\log(L/L_{\odot}) = 2.00 \pm 0.09$ , is very close to the value  $\log(L/L_{\odot}) = 2.06$  determined by Aurière et al. (2007). The fundamental

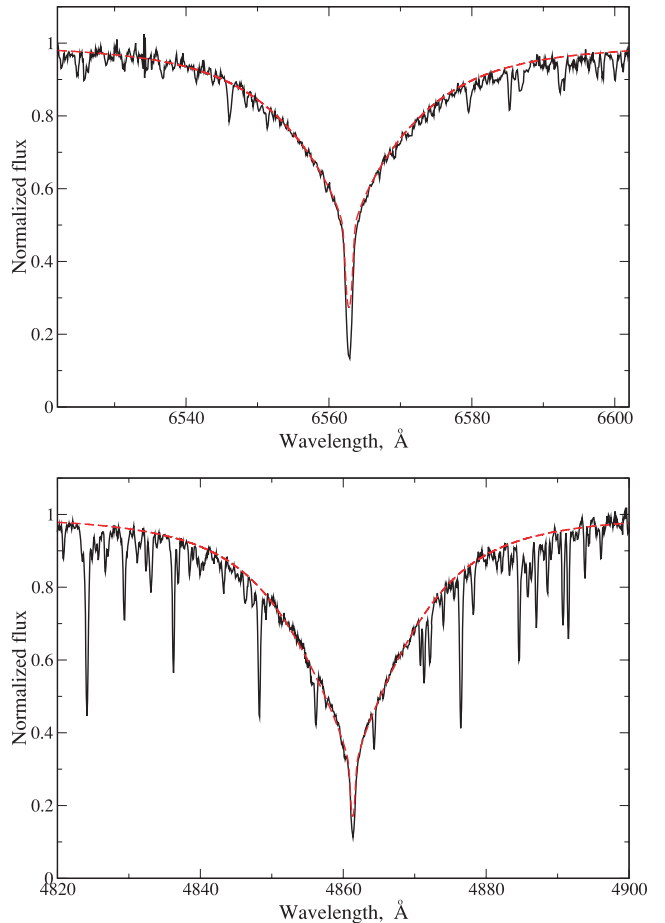


**Figure 4.** Comparison between the observed and synthesized H $\alpha$  (top) and H $\beta$  (bottom) line profiles for a model atmosphere with  $T_{\text{eff}} = 9500$  K,  $\log g = 3.6$ ,  $M = +0.5$ .

parameters of HD 103498, as well as its chemical peculiarities (see next section), are very similar to those of the evolved Ap stars HD 133792 (Kochukhov et al. 2006) and HD 204411 (Ryabchikova, Leone & Kochukhov 2005). The position of HD 103498 on the HR diagram (see Fig. 8) provides additional support for the lower gravity derived from hydrogen-line profiles as compared to photometric calibrations.

### 3.2.2 Atmospheric abundances

The identification of lines in the spectrum of HD 103498 was based on the theoretical spectrum calculated for the entire observed spectral region using the line extraction from VALD (Kupka et al. 1999 and references therein) and DREAM (Biémont, Palmeri & Quinet 1999) data bases. Atomic data on the rare-earth elements (REE) compiled in the DREAM data base were extracted via the VALD interface. Comparison of the synthetic and observed spectra allowed us to choose the least blended lines for the abundance analysis. Direct comparison of the HD 103498 spectrum with the spectrum of the well-studied Ap star HD 133792 (Kochukhov et al. 2006) shows a pronounced similarity between the two objects: both spectra are

crowded with strong lines of Fe-peak elements, whereas the lines of the REE are weak or absent. Cr II and Fe II lines with the lower-level excitation energy above 10 eV are numerous and many of them are strong, which is an indication of the extreme Cr and Fe overabundances in the stellar atmospheres.

Local thermodynamic equilibrium abundance determination is based mainly on the equivalent widths analysed with the improved version of WIDTH9 code updated for the VALD output line lists and kindly provided by V. Tsymbal. Model atmosphere was calculated with the ATLAS9 code (Kurucz 1993) using a metallicity  $[M/H] = +0.5$ . To make a proper selection of unblended and minimally blended lines for abundance calculations we synthesized the whole observed spectral region 3965–7270 Å with the help of the SYNTH3 code (Kochukhov 2007). The best fit to the observed unblended line profiles was achieved for  $v_e \sin i = 12 \text{ km s}^{-1}$ , in close agreement with the  $v_e \sin i = 13 \text{ km s}^{-1}$  derived by Aurière et al. (2007) from the mean metal line profile. Microturbulent velocity,  $\xi_t = 1.0 \pm 0.2 \text{ km s}^{-1}$ , was obtained as an averaged value between the values derived from numerous lines of Cr I, Cr II, Fe I and Fe II. Table 2 summarizes the results of our abundance analysis. For each species an average abundance with rms based on ‘ $n$ ’ measured lines is

**Table 2.** Local thermodynamic equilibrium atmospheric abundances of HD 103498 with the error estimates based on the internal scattering from the number of analysed lines,  $n$ . The fourth and fifth columns give abundances in similar stars, HD 133792 and HD 204411, for comparison. The last column gives the abundances of the solar atmosphere (Asplund et al. 2005).

Ion	HD 103498 $\log(N/N_{\text{tot}})$	$n$	HD 133792 $\log(N/N_{\text{tot}})$	HD 204411 $\log(N/N_{\text{tot}})$	Sun $\log(N/N_{\text{tot}})$
Cr I	$-4.11 \pm 0.23$	3	-4.68	-4.37	-3.65
O I	-3.92:	1	-4.23	-4.03	-3.38
Na I	-5.09:	1	-5.35	-5.28	-5.87
Mg I	$-3.58 \pm 0.13$	4	-3.91	-4.34	-4.51
Mg II	$-4.43 \pm 0.27$	3	-4.18	-4.62	-4.51
Al II	-6.06:	1	-6.03	-5.85	-5.67
Si I	$-3.65 \pm 0.33$	3	-3.69	-4.13	-4.53
Si II	$-3.64 \pm 0.47$	5	-5.09	-4.11	-4.53
Ca II	-5.91	1	-7.36	-4.67	-5.73
Ti II	$-6.45 \pm 0.16$	15	-6.88	-6.49	-7.14
V II	$-8.14 \pm 0.18$	2	-8.14		-8.04
Cr I	$-3.25 \pm 0.23$	71	-3.79	-4.85	-6.40
Cr II	$-3.31 \pm 0.24$	151	-3.75	-4.70	-6.40
Mn I	$-5.94 \pm 0.11$	2	-5.55	-5.96	-6.65
Mn II	$-5.72 \pm 0.23$	3	-5.39	-5.66	-6.65
Fe I	$-2.98 \pm 0.20$	80	-3.31	-3.76	-4.59
Fe II	$-3.01 \pm 0.18$	169	-3.18	-3.52	-4.59
Co II	-5.58:	1	-5.99	-6.50	-7.12
Ni I	-5.34:	1	-6.05	-5.68	-5.81
Sr II	$\leq -8.5$	3	-6.36	-8.5:	-9.12
Ba II	-8.64:	1	-8.73	-9.02	-9.87
Ce II	-9.10:	1	-9.07:	-10.26	-10.46
Pr III	$-8.87 \pm 0.33$	4	-9.51	$< -10.5$	-11.33
Nd III	$-8.41 \pm 0.16$	9	-9.08	-10.05	-10.59
Sm II	-8.70:	1	$\leq -10.4$		-11.03
Eu II	$-8.85 \pm 0.12$	2	-9.81	-10.95	-11.53
Gd II	-8.72:	1	-9.60		-10.92
$T_{\text{eff}}$	9500 K		9400 K	8400 K	5777 K
$\log g$	3.6		3.7	3.5	4.44
$\xi_t$	$1.0 \text{ km s}^{-1}$		$0.0 \text{ km s}^{-1}$	$0.0 \text{ km s}^{-1}$	$0.9 \text{ km s}^{-1}$
$v_e \sin i$	$12 \text{ km s}^{-1}$		$1.0 \text{ km s}^{-1}$	$6.3 \text{ km s}^{-1}$	$1.9 \text{ km s}^{-1}$
$\log(L/L_{\odot})$	2.00		2.02	2.01	
$\langle B_z \rangle, G$	169		120	88	

given. For comparison we also give abundances in the atmospheres of two CrFe-rich evolved Ap stars, HD 133792 (Kochukhov et al. 2006) and HD 204411 (Ryabchikova et al. 2005), and in the solar photosphere (Asplund, Grevesse & Sauval 2005).

The results show that HD 103498 has the largest Cr and Fe overabundances among the three stars. It is also Si-overabundant, but silicon seems to be stratified similarly to in HD 133792 and HD 204411. Calcium lines are weak, and we analysed only one Ca II line,  $\lambda$  6456.88. Trying to fit the resonance Ca II  $\lambda$  3933.66 line the fit to the line core requires 10 times smaller abundance than inferred from the wings and from the  $\lambda$  6456.88 line. This indicates the presence of Ca stratification similar to that in HD 133792 (Kochukhov et al. 2006) and in HD 204411 (Ryabchikova et al. 2005). We also found that the core of Ca II  $\lambda$  3933.66 is blue-shifted by  $\sim 0.02$  Å. Blue shift of this line was also found in HD 133792, which is known to have a strong Ca isotopic anomaly (see Ryabchikova, Kochukhov & Bagnulo 2008, Section 6). To investigate the Ca isotopic anomaly in HD 103498 spectral observations in the region of the IR Ca II triplet, which has the largest isotopic separation, are needed.

Spectral synthesis of the regions around the resonance Sr II  $\lambda\lambda$  4077, 4215 as well as Sr II  $\lambda$  4305 lines clearly shows that lines of Cr and Fe, not of Sr II, provide the main contribution to the observed strong features appearing at the position of the Sr II lines. In fact, the Sr abundance in HD 103498 does not much exceed the solar one. Thus, classification of Cr-rich stars as Cr-Sr based on low-resolution spectra may be incorrect. Furthermore, it is interesting to note that the two stars with substantial rotation, HD 103498 and HD 204411, have the same small Sr overabundance, whereas HD 133792, with negligible rotation, is very Sr-overabundant but is similar to the other two stars in the abundances of other elements.

### 3.3 Cross-correlation radial velocity analysis

Owing to the substantial difference of the atmospheric parameters and spectral appearance of HD 103498 from those of other known roAp stars, we do not have any a priori information on which lines might be most suitable for the detection of velocity oscillations. In this situation, a cross-correlation analysis of large spectral regions appears to be the optimal approach to the spectroscopic search for pulsations. In roAp stars, metal lines exhibit a large scatter in the pulsation amplitude and phase, leading to a significant dilution of the signal coming from strongly pulsating lines by lines showing weak or no variation. However, even in this case cross-correlation studies are usually successful in detecting oscillation signals with amplitudes as low as a few metres per second (e.g. Hatzes & Mkrtychian 2004).

We applied the cross-correlation analysis to the individual echelle orders of the FIES spectra of HD 103498. The time-resolved spectra were compared with the mean one using the chi-square criterion, and the RV shift minimizing the chi-square was recorded. Only the spectral regions containing absorption features deeper than 3 per cent were included in the analysis. The RV curves obtained with this method were analysed using the standard discrete Fourier transform (FT) technique. Fig. 5 shows the amplitude spectra for seven consecutive echelle orders in the spectral region characterized by a high signal-to-noise ratio and a high line density. No statistically significant periodicity is evident. The highest noise peaks reach  $15\text{--}20$  m s $^{-1}$ . We also analysed a mean RV curve obtained by combining the measurements for 16 echelle orders for which the best RV precision was achieved. The corresponding FT spectrum is shown in the lower right panel of Fig. 5. It reveals no oscillations stronger than  $\approx 5$  m s $^{-1}$ . The upper limit for the pulsations

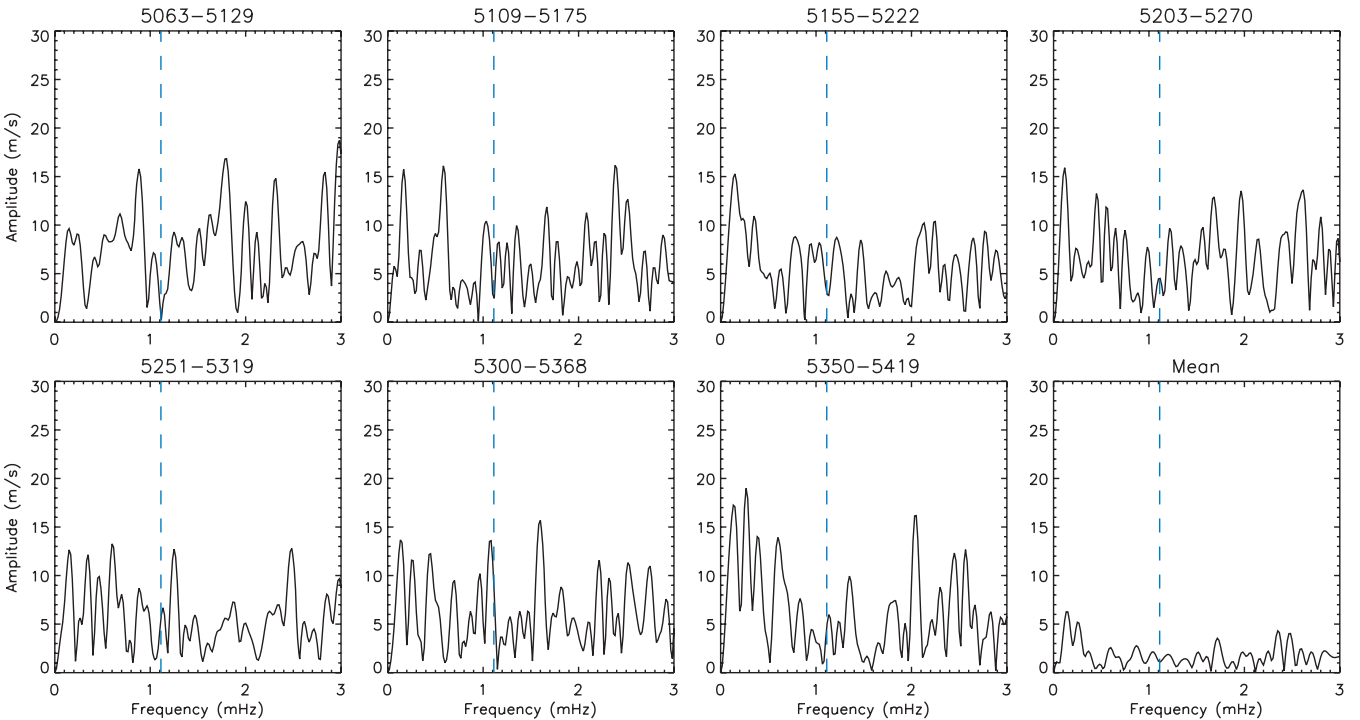


**Figure 5.** Amplitude spectra of the cross-correlation radial velocity measurements for seven representative echelle orders of the FIES spectra of HD 103498. The lower right panel shows the amplitude spectrum for velocity obtained by combining radial velocity curves of the 16 best orders. The vertical dashed line indicates the mean frequency identified in photometric observations.



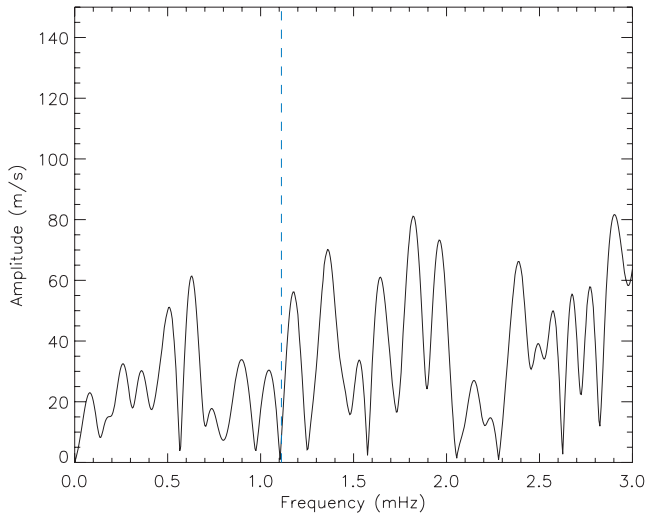


**Figure 6.** Amplitude spectrum of the centre-of-gravity radial velocity measurements averaged for eight lines of Pr III and Nd III in HD 103498. The vertical dashed line indicates the mean frequency identified in photometric observations.

in the vicinity of the photometric frequency of HD 103498 is only  $2.8 \text{ m s}^{-1}$ .

In most roAp stars, the lines of the REE in the first and second ionization stages usually show the highest RV amplitudes. In HD 103498 these lines are either virtually absent (REE II) or weak (REE III), whereas the lines of Fe-peak elements are numerous and strong. Therefore, a pulsation signal from the REE lines may be lost in cross-correlation analysis. We made centre-of-gravity RV measurements of the individual lines of Pr III  $\lambda\lambda$  5300, 6867 and Nd III  $\lambda\lambda$  4914, 4927, 5050, 5102, 5294, 6327, and analysed the resulting mean RV curves for the two REE species. The corresponding FT spectrum, shown in Fig. 6, provides no evidence of the RV pulsation signal in the vicinity of the photometric frequency. However, the upper limit of the pulsation amplitude is fairly large,  $\approx 80 \text{ m s}^{-1}$ .

#### 4 DISCUSSION

The detection of 15-min periodic oscillations in the photometric data of 2007 followed by non-detection in the spectroscopic data of 2009 is of vast importance. The possible reason for this phenomenon may be significant intrinsic changes of the stellar pulsational amplitude. The absence of periodic light variations in the photometric data sets from 2006, 2008 and 2009 could be caused by the fact that the real amplitude variations might be buried under the noise. The detection limit of the photometric variability depends on the atmospheric noise, which consists of the scintillation noise and long-term sky-transparency variations. Fig. 7 shows the average atmospheric noise at ARIES observatory based on the high-speed photometric observations carried out under the ‘Nainital-Cape Survey’ project aimed at searching for and studying pulsational variability in chemically peculiar stars (Martinez et al. 2001; Joshi et al. 2006, 2009). The fitted solid line corresponds to the Fourier transform of the light curves of 47 stars observed on 84 occasions during 1999–2000, and the dotted line is for 21 stars observed on 33 occasions during 2008–2009. The respective amplitudes of the sky-transparency variations and scintillation noise in the year 1999–2000 are 7.23 and 0.50 mmag, and the corresponding values for the year 2008–2009 are 11.68 and 0.66 mmag, respectively. This clearly shows that the atmospheric noise has increased slightly during the last 10 years

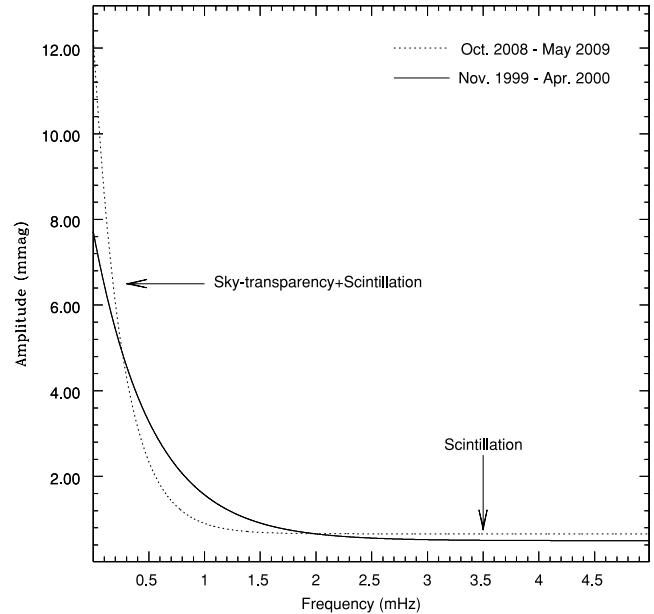


**Figure 7.** The average sky-transparency and scintillation noise obtained by analysis of high-speed photometric observations for 1999–2000 (solid line) and 2008–2009 (dotted line). The scintillation noise appears at higher frequencies ( $> 1 \text{ mHz}$ ), which sets the limit of detection of high-overtone pulsations (roAp-like oscillations). The long-term sky-transparency variations occur at lower frequencies ( $< 1 \text{ mHz}$ ), where it is very difficult to distinguish the low-overtone pulsations ( $\delta$  Scuti-type) from the sky-transparency variations.

owing to increased human activity around the observatory. The atmospheric noise can be minimized by installing bigger telescopes at a good observing site where the sky is stable and photometric (Young 1967). With this in mind, ARIES is now in the process of installing 1.3-m and 3.6-m optical telescopes at a new astronomical site, Devasthal (longitude:  $79^{\circ}40'57''\text{E}$ , latitude:  $29^{\circ}22'26''\text{N}$ , altitude: 2420 m), due to be completed by the end of 2009 and 2012, respectively. This site has an average seeing of  $\approx 1$  arcsec near the ground and  $\approx 0.65$  arcsec at 12 m above the ground (Sagar et al. 2000; Stalin et al. 2001). In the near future, the new observing facilities at Devasthal will make a significant contribution in the area of asteroseismology.

It is possible to attribute the non-detection of pulsations in the spectroscopy to observation at an unfavorable rotation phase,  $\varphi \approx 0.25$  or  $0.75$ , when the magnetic equator passes in front of the observer. Unfortunately, the magnetic ephemeris of HD 103498 is not known with a high enough accuracy to establish the precise rotational phase of our observations. On the other hand, we do not observe clear modulation of the photometric pulsational amplitude on the time-scale of the rotation period, which argues against such modulation in spectroscopy. Furthermore, spectroscopic studies of a few roAp stars that were followed over the entire rotation cycle (e.g. Kochukhov 2004; Mkrtchian & Hatzes 2005) show that RV pulsation never disappears entirely.

Fig. 8 shows the position of HD 103498 on the HR diagram, where an instability strip for roAp stars is indicated (Cunha 2002). For comparison, positions of two evolved Ap stars, HD 133792 and HD 204411, are shown. The stellar evolutionary tracks for the mass range from  $1.5$  to  $2.7 M_{\odot}$  (Christensen-Dalsgaard 1993) are also over-plotted. Pulsation calculations by Cunha (2002) and a more recent theoretical study by Théado et al. (2009) predict the excitation of pulsations in relatively hot and more evolved Ap stars. However,

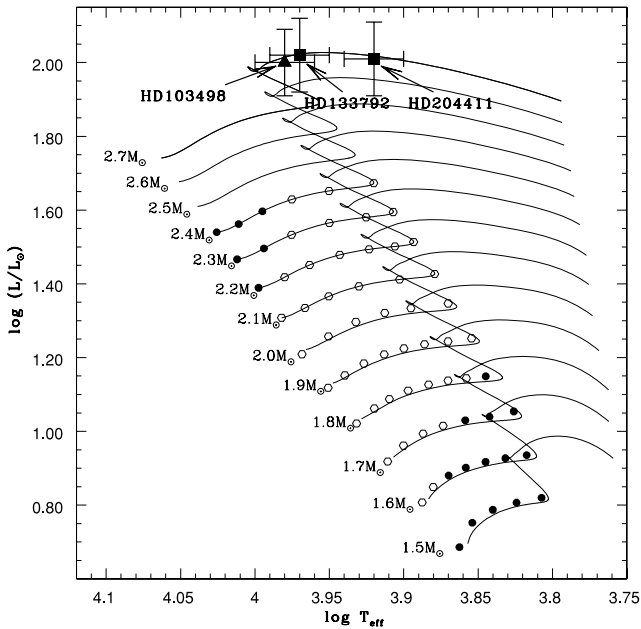


**Figure 8.** HR diagram showing the position of HD 103498 (black triangle), having  $T_{\text{eff}} = 9500 \pm 200$  K and  $\log(L/L_{\odot}) = 2.0$ . For comparison, the positions of two evolved Ap stars, HD 133792 and HD 204411, having  $T_{\text{eff}} = 9400 \pm 190$  K and  $\log(L/L_{\odot}) = 2.02$  and  $T_{\text{eff}} = 8400 \pm 200$  K and  $\log(L/L_{\odot}) = 2.01$ , respectively, are shown (black squares). The filled circles show radiative envelope models in which no high-order acoustic oscillations were found, and the open circles show the models in which the latter were found.

all of about 40 currently known roAp stars have temperatures in the  $T_{\text{eff}}$  interval from 6400 to 8100 K. The search for RV pulsations in evolved stars with  $T_{\text{eff}}$  larger than 8100 K was not successful (Freyhammer et al. 2008). If confirmed, the discovery of pulsations in HD 103498 with  $T_{\text{eff}} = 9500$  K may have a profound consequence for our understanding of the excitation of  $p$ -modes in magnetic Ap stars.

## 5 CONCLUSIONS

The time-series photometric observations of HD 103498 taken on five nights show a clear pulsational variability of about 15 min with amplitude modulation. However, this periodicity could not be confirmed in follow-up photometric and high-resolution spectroscopic observations. Hence, the pulsational variability in HD 103498 should be considered with caution. The abundance analysis of HD 103498 shows that the lines of the rare-earth elements – the best indicators of RV pulsations in roAp stars – are fairly weak. It is also observed that the core of  $\text{Ca II } \lambda 3933.66$  is blue-shifted by  $\sim 0.02$  Å, which may be a result of anomalous Ca isotopic composition. The cross-correlation RV analysis revealed no oscillations with amplitudes above  $\approx 5$  m s $^{-1}$ . The measurements of the centre of gravity of eight individual REE lines also did not show any evidence of an RV pulsation signal in the vicinity of the photometric frequency. More time-series photometric and spectroscopic observations are required to study the variable nature of HD 103498.

## ACKNOWLEDGMENTS

The authors are grateful to Professor Ram Sagar for encouragement to initiate the Indo-Russian collaboration. We thank Dr G. Wade

for providing the MuSiCoS spectra of HD 103498, and the NOT telescope staff for helping to collect the spectra of HD 103498. We thank the reviewer, Dr Pierre North, for useful comments and suggestions, which led to significant improvements in the manuscript. Resources provided by the electronic data bases (VALD, SIMBAD, NASA's ADS) are acknowledged. This work was supported by the Presidium RAS program, by a research grant from the RFBI (08-02-00469a), by the Russian Federal Agency on Science and Innovation (02.740.11.0247), INT/ILTP/B-3.19 and INT/ILTP/B-3.16. OK is a Royal Swedish Academy of Sciences Research Fellow supported by a grant from the Knut and Alice Wallenberg Foundation. Part of this work was carried out under the Indo-South Africa Science and Technology Cooperation (INT/SAFR/P-04/2002/13-02-2003 and INT/SAFR/P-3(3)2009) funded by the Departments of Science and Technology of the Indian and South African governments. SJ acknowledges his colleagues for the critical reading of the manuscript.

The spectroscopic observations were made from the Nordic Optical Telescope operated on the island of La Palma jointly by Denmark, Finland, Iceland, Norway and Sweden, in the Spanish Observatorio del Roque de los Muchachos of the Instituto de Astrofísica de Canarias.

## REFERENCES

- Abt H. A., Morrell N. I., 1995, *ApJS*, 99, 135  
 Ashoka B. N., Kumar, Babu V. C., Seetha S., Girish V., Gupta S. K., Sagar R., Joshi S., Narang P., 2001, *JA&A*, 22, 131  
 Asplund M., Grevesse N., Sauval A. J., 2005, in Barnes T. G., III, Bash F. N., eds, *ASP Conf. Ser. Vol. 336, Cosmic Abundances as Records of Stellar Evolution and Nucleosynthesis*. Astron. Soc. Pac., San Francisco, p. 25  
 Aurière M. et al., 2007, *A&A*, 475, 1053  
 Biémont E., Palmeri P., Quinet P., 1999, *Ap&SS*, 269–270, 635  
 Christensen-Dalsgaard J., 1993, in Weiss W. W., Baglin A., eds, *ASP Conf. Ser. Vol. 40, Inside the Stars*, IAU Colloq. 137. Astron. Soc. Pac, San Francisco, p. 483  
 Cunha M., 2002, *MNRAS*, 333, 47  
 Deeming T. J., 1975, *Ap&SS*, 36, 137  
 Freyhammer L. M., Kurtz D. W., Cunha M. S., Mathys G., Elkin V. G., Riley J. D., 2008, *MNRAS*, 385, 1402  
 Glagolevskij Yu. V., Bychkov V. D., Romanyuk I. I., Chunakova N. M., 1985, *Bull. Spec. Astrophys. Obs.*, 19, 26  
 Hatzes A. P., Mkrtrichian D. E., 2004, *MNRAS*, 351, 663  
 Hauck B., Mermilliod M., 1998, *A&AS*, 129, 431  
 Huchra J., Willner S. P., 1973, *PASP*, 85, 85  
 Joshi S., Mary D. L., Martinez P., Kurtz D. W., Girish V., Seetha S., Sagar R., Ashoka B. N., 2006, *A&A*, 455, 303  
 Joshi S., Mary D. L., Chakradhari N. K. Tiwari S. K. Billaud C., 2009, *A&A*, in press (arXiv:0909.0810)  
 Kaiser A., 2006, in Sterken C., Aerts C., eds, *ASP Conf. Ser. Vol. 349, Astrophysics of Variable Stars*. Astron. Soc. Pac., San Francisco, p. 257  
 Kochukhov O., 2004, *A&A*, 446, 1051  
 Kochukhov O., 2007, in Kudryavtsev D. O., Romanyuk I. I., eds, *Physics of Magnetic Stars. Special Astrophysical Observatory, Nizhnij Arkhyz*. p. 109  
 Kochukhov O., Tsymbal V., Ryabchikova T., Makaganyk V., Bagnulo S., 2006, *A&A*, 460, 831  
 Kochukhov O., Ryabchikova T., Weiss W. W., Landstreet J. D., Lyashko D., 2007, *MNRAS*, 376, 651  
 Kochukhov O., Bagnulo S., Lo Curto G., Ryabchikova T., 2009, *A&A*, 493, L45  
 Kunzli M., North P., Kurucz R. L., Nicolet B., 1997, *A&AS*, 122, 51  
 Kupka F., Piskunov N., Ryabchikova T. A., Stempels H. C., Weiss W. W., 1999, *A&AS*, 138, 119



- Kurucz R. L., 1993, Kurucz CD-ROM No. 13. Smithsonian Astrophysical Observatory, Cambridge, MA
- Martinez P. et al., 2001, *A&A*, 371, 1048
- Mkrtychian D. E., Hatzes A. P., 2005, *A&A*, 430, 263
- Moon T. T., Dworetzky M. M., 1985, *MNRAS*, 217, 305
- Piskunov N. E., Valenti J. A., 2002, *A&A*, 385, 1095
- Pourbaix D. et al., 2004, *A&A*, 424, 727
- Runefer F., 1976, *A&AS*, 26, 275
- Ryabchikova T., Kochukhov O., Bagnulo S., 2008, *A&A*, 480, 811
- Ryabchikova T., Leone F., Kochukhov O., 2005, *A&A*, 438, 973
- Sagar R., 1999, *Current Sci.*, 77, 643
- Sagar R. et al., 2000, *A&AS*, 144, 349
- Scargle J. D., 1982, *ApJ*, 263, 835
- Stalin C. S. et al., 2001, *BASI*, 2001, 29, 39
- Théado S., Dupret M.-A., Noels A., Ferguson J. W., 2009, *A&A*, 493, 159
- Tiwari S. K., Chaubey U. S., Pandey C. P., 2007, *Inf. Bull. Var. Stars*, No. 5900
- van Leeuwen F., 2007, *A&A*, 474, 653
- Young A. T., 1967, *AJ*, 72, 747

This paper has been typeset from a  $\text{\TeX}/\text{\LaTeX}$  file prepared by the author.